

Syracuse University

## SURFACE at Syracuse University

---

Renée Crown University Honors Thesis Projects Syracuse University Honors Program Capstone  
- All Projects

---

Spring 5-1-2019

### Modification of Calmodulin EF Hands for Rare Earth Metal Selectivity

Alaine Gigon

Follow this and additional works at: [https://surface.syr.edu/honors\\_capstone](https://surface.syr.edu/honors_capstone)



Part of the [Biology Commons](#)

---

#### Recommended Citation

Gigon, Alaine, "Modification of Calmodulin EF Hands for Rare Earth Metal Selectivity" (2019). *Renée Crown University Honors Thesis Projects - All*. 1344.

[https://surface.syr.edu/honors\\_capstone/1344](https://surface.syr.edu/honors_capstone/1344)

This Honors Capstone Project is brought to you for free and open access by the Syracuse University Honors Program Capstone Projects at SURFACE at Syracuse University. It has been accepted for inclusion in Renée Crown University Honors Thesis Projects - All by an authorized administrator of SURFACE at Syracuse University. For more information, please contact [surface@syr.edu](mailto:surface@syr.edu).

Modification of Calmodulin EF Hands for Rare Earth Metal Selectivity

A Capstone Project Submitted in Partial Fulfillment of the  
Requirements of the Renée Crown University Honors Program at  
Syracuse University

Alaine Gigon

Candidate for Bachelor of Science  
and Renée Crown University Honors  
Spring 2019

Honors Capstone Project in Biology

Capstone Project Advisor: \_\_\_\_\_  
Professor Ivan Korendovych

Capstone Project Reader: \_\_\_\_\_  
Professor Melissa Pepling

Honors Director: \_\_\_\_\_  
Dr. Danielle Smith, Director

## Abstract

Positron Emission Tomography and Magnetic Resonance Imaging, two of the most clinically important imaging techniques, often rely on the ability to bind lanthanide ions with high affinity. Small, non-immunogenic metal-binding proteins with a high affinity for lanthanides have been highly sought out for such purposes due to low likelihood for immunogenicity, versatility, and ease of modification<sup>3</sup>. However, despite much effort the problem of creating proteins for specific and selective binding of lanthanides *a la carte* has not been solved.

Our approach is to engineer catalytic sites into existing metal-binding proteins to link metal binding to a straightforward spectroscopic readout. Calmodulin (CaM), a eukaryotic messenger protein, binds  $\text{Ca}^{2+}$  through its EF-hands, initiating a conformational change that forms an active site for substrate binding<sup>1</sup>. Previous experiments within the Korendovych lab converted CaM into AlleyCat7, a highly efficient enzyme for Kemp elimination, a reaction that can be followed visually<sup>2</sup>. Here we report that by strategically introducing two mutations into AlleyCat7, it can be converted into a selective binder of lanthanides. The resulting protein, named HolLEE, is at least 10,000-fold more selective for lanthanides as compared to  $\text{Ca}^{2+}$ , an ion normally present in blood at high concentrations. We are particularly interested in yttrium-binding properties of HolLEE, due to importance of  $^{90}\text{Y}$  as a theranostic nucleus for treatment of Hepatocellular Carcinoma (HCC). In addition to biomedical applications HolLEE can serve as a biocompatible, catalytically-amplified sensor for metal ions.

## Executive Summary

The project *Modification of Calmodulin EF Hands for Rare Earth Metal Selectivity* was conducted to develop a protein-based sensor, based on the scaffold of the protein calmodulin, that is capable of binding lanthanide ions, and most importantly yttrium. Through utilizing site-directed mutagenesis, the most current generation of the calmodulin-based protein AlleyCat7 was modified into HolLEE. Altering the aspartates in the 95 and 131 positions into glutamates enabled the intended ion binding, all while rejecting the native binding nature of calmodulin to calcium ions. Once these modifications were made the catalytic nature of HolLEE was confirmed by its ability to perform kemp elimination, a reaction which lead to trackable spectroscopic read-out. After confirming the catalytic ability of HolLEE subsequent testing was done to determine which ions enable the highest level of catalytic activity, which ions contributed to protein stability, and that HolLEE was capable of being conjugated to the antibody 2E10 while maintaining its catalytic abilities. HolLEE will have the potential to be applied in vivo to treat hepatocellular carcinoma, a cancer that mainly affects the liver.

The basis for our protein mutant HolLEE is the protein calmodulin. Calmodulin is a commonly found in the human body, and through its interactions with the calcium in its ionic form it enables biological interactions in the muscular and nervous system at the cellular level<sup>3</sup>. Calmodulin was also chosen as the scaffold for HolLEE due to previous success in implementing catalytic ability by way of reformatting its structure by way of site directed mutagenesis<sup>1</sup>. This technique consists of altering the DNA sequence of the protein at the codon level, so once it is transcribed and translated there will be direct changes in the amino acid sequence, and consequently the structure of the protein. Such changes were done in order to change the shape of allosteric site present near positions 95 and 131, in order reject the binding of the calcium ion,

and ensure any catalytic ability was the result of binding with lanthanide ions and/or yttrium.

Success of these changes were tracked by way of HolLEE's ability to perform the kemp elimination reaction. Kemp elimination is a useful reaction in the biochemical industry, because upon kemp binding to a biocatalyst, there will be a spectroscopic signal at 380nm that can be detected. The plate reader then provides a value that can be correlated to the amount of product turned over by the catalyst, known as  $k_{cat}$ . The data provided from the plate reader can also be derived to get the  $k_m$  value, which is when the enzyme reaches half of its maximum velocity. When one divides  $k_{cat}/k_m$ , the value produced corresponds directly to the catalyst's catalytic efficiency. The higher catalytic efficiency is for a catalyst, the more effective it is at creating the desired product in a timely manner.

These concepts were applied to assessing the effectiveness of HolLEE by way of kinetic assays, metal dependence assays, and circular dichromism (CD) spectroscopy. Kinetic assays were performed in order to determine the optimum substrate: protein ratio that would lead to the highest catalytic efficiency. The metal dependence assays were conducted in order to determine which of the lanthanide ions and/or yttrium would produce the highest rate of catalytic efficiency, and the optimum metal: protein concentration ratio. CD spectroscopy was done in order to see how the binding of certain metals would affect the stability of the protein HolLEE. This form of light absorption spectroscopy reveals the characteristics of a protein samples secondary structure, such as the content of alpha helixes and beta sheets, by way calculating the difference in absorbance right- and left-circularly polarized light. Once these methods were applied to confirm the stability and catalytic nature of HolLEE upon binding the metal yttrium, the protein was then conjugated to the anti-cancer antibody 2E10 to form the preliminary in vitro theranostic 2E10-HolLEE<sup>12</sup>. After the conjugate was formed, it endured kinetic assays which

compared its efficiency upon binding yttrium and select lanthanides, to an unconjugated form of HolIEE which bound the same ions. While it was found that the unconjugated form of HolIEE retained higher levels of catalytic efficiency comparatively to its conjugated counter-part, the retainment of a fraction of the original catalytic efficiency for 2E10-HolIEE is a step in the right direction.

Research such as mine in the Korendovych lab is centered in the field of biochemistry, and using protein engineering to develop biocatalysts that have the potential of medical application. Protein engineering in this project capitalizes upon utilizing the protein calmodulin as the basis of a theranostic, a singular agent that is capable of being utilized for diagnosis, drug delivery, and treatment<sup>10</sup>. Being a protein native to the human body, if implanted as a <sup>90</sup>Y theranostic HolIEE poses a low threat of inducing an immunological response that would be harmful to the patient. HolIEE showed the ability to bind to a wide-array of lanthanide ions, such as the common radionuclide gadolinium, all while maintaining catalytic ability. This means HolIEE also has the potential to be utilized to treat cancers other than HCC. HolIEE has been easy to manufacture, modify, and is greatly versatile. HolIEE holds great promise as a biocatalyst that can be utilized in the medical field and other fields, such as the environmental industry, which rely upon the ability of biological molecules to bind radioactive substances.

## Table of Contents

<b>Abstract.....</b>	<b>1</b>
<b>Executive Summary .....</b>	<b>2-4</b>
<b>Acknowledgements.....</b>	<b>6</b>
<b>Chapter 1: Background.....</b>	<b>7</b>
<b>Chapter 2: Timeline.....</b>	<b>19</b>
<b>Chapter 3: Methods.....</b>	<b>20</b>
<b>Chapter 4: Experimentals.....</b>	<b>24</b>
<b>Chapter 5: Discussion.....</b>	<b>33</b>
<b>Works Cited.....</b>	<b>36</b>

## **Acknowledgements**

I am thankful for the never-ending amount of support I received through my life from my parents, brother, and those I see in my eyes as family. It is through their love I feel empowered to push myself to be better academically and as a person, in order to achieve my goal of making the world a better place for everyone through science and medicine. I am thankful for the Syracuse Army ROTC program for allowing me to not only attend this great university, but for putting me on a path to serve my country as a leader in medicine. I would like to thank my laboratory advisors Ivan Korendovych and Olga Makhlynets for providing me with the great opportunity to contribute to research I know that will help change lives for the better. I thank you for my lab mates, especially Michelle Takacs and Joel Rempillo, for helping me apply and expand my scientific knowledge and skills in a meaningful way, as well as all humor and fun we shared along the way.

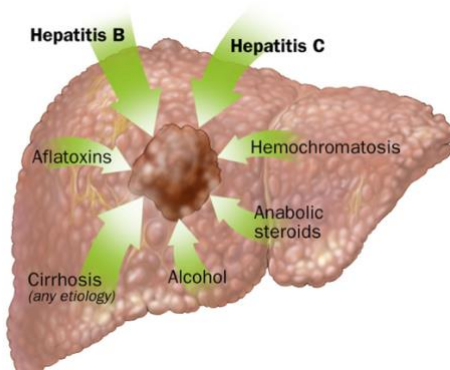


## Background

The ability to sense metals has vital scientific application ranging from tracking metal ions within the natural environment to being able to determine metal concentration at the cellular level. Current methods for developing molecular metal sensors have proven to be costly, challenging to create, and are prone to being incompatible with living systems. Protein-based sensors have paved a new era for biocompatible, as well as biodegradable, sensors that through allosteric reactions, may express as a trackable fusion tag for metal ions *in vivo*<sup>3</sup>.

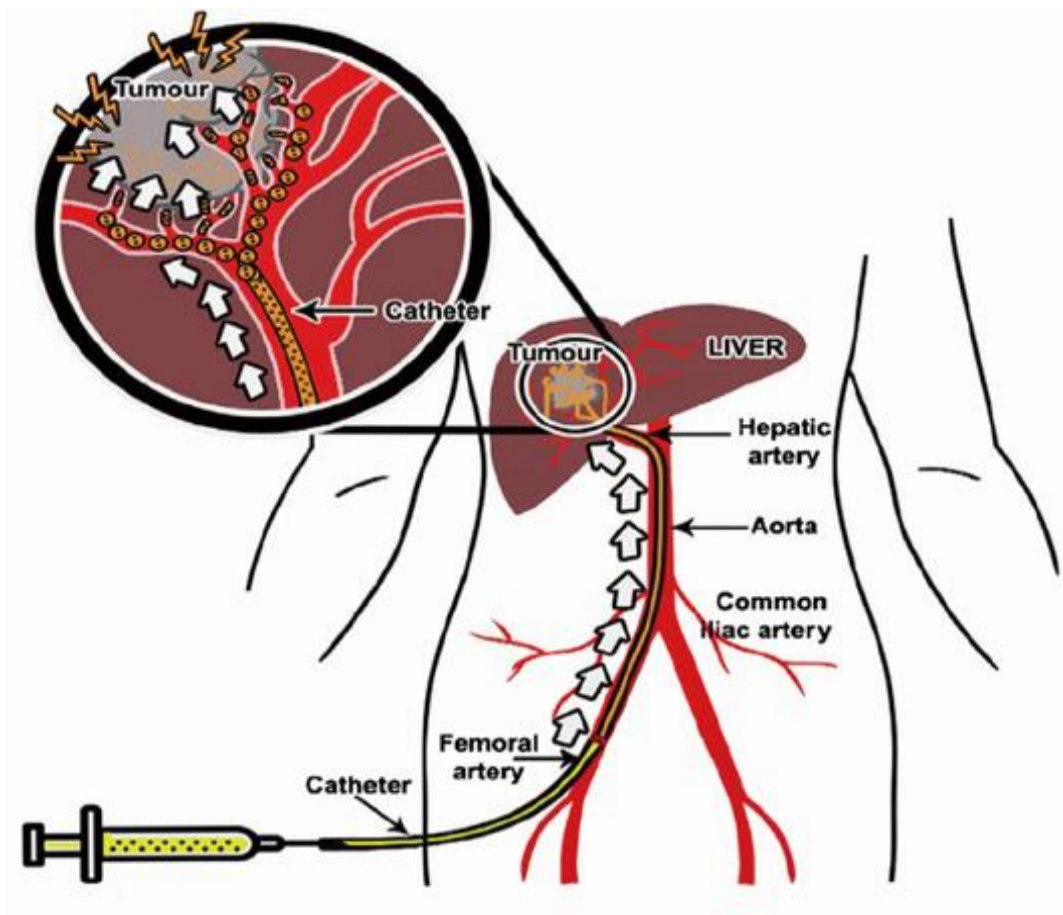
The Korendovych Lab is interested in developing protein-based sensors with the ultimate purpose of detecting hepatocellular carcinoma (HCC). HCC is a cancer that can be caused by the cirrhosis of the liver, hepatitis infection, aflatoxins, anabolic steroids, alcohol, and hemochromatosis, as seen in figure 1<sup>6</sup>. In the world HCC is the fifth most diagnoses cancer, and third most deadly with a 94% death rate within five years of diagnosis<sup>6</sup>. Detection is difficult due to the lack of symptoms of the illness, and inadequate equipment. For example, MRI is not a viable option if the patient has metallic implants, and PET imaging is unable to differentiate HCC cells from noncancerous hepatic cells in the early stages of the disease when intervention is most useful<sup>7</sup>.

**Figure 1: Causes of HCC in the liver<sup>6</sup>**



As to how HCC is currently treated the most popular method is transarterial chemoembolization (TACE). As one can see in figure 2 order to conduct TACE therapy a catheter is fed through the hepatic artery to deliver medication directly to the blood supply of the tumor. One of the most common drugs used with this technique is  $^{90}\text{Y}$  microspheres that release radiation to kill the tumor cell directly. This technique can be very effective in reducing the size of tumors but cannot be used if the tumor is not of sufficient size or has spread to another part of the body<sup>6</sup>.

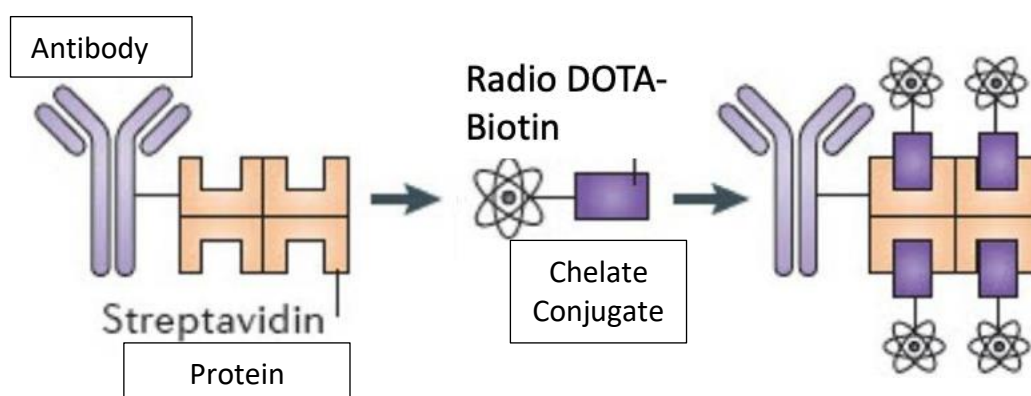
**Figure 2: TACE Treatment**



Radioimmunotherapy is a common therapy for many cancers, yet has not been greatly applied to HCC treatment. In Radioimmunotherapy an antibody labeled with a radionuclide can be attached directly to the antibody or by use of a chelate, which is an organic molecule that can

directly bind metal at two or more points, is used to deliver cytotoxic radiation to a target cell. In figure 3 we see the protein streptavidin when conjugated to an antibody can bind four radio-DOTA-biotin moieties, amplifying tumor-targeted radioactivity<sup>8</sup>. Such treatment has been successful in targeting neuroendocrine and prostate cancers.

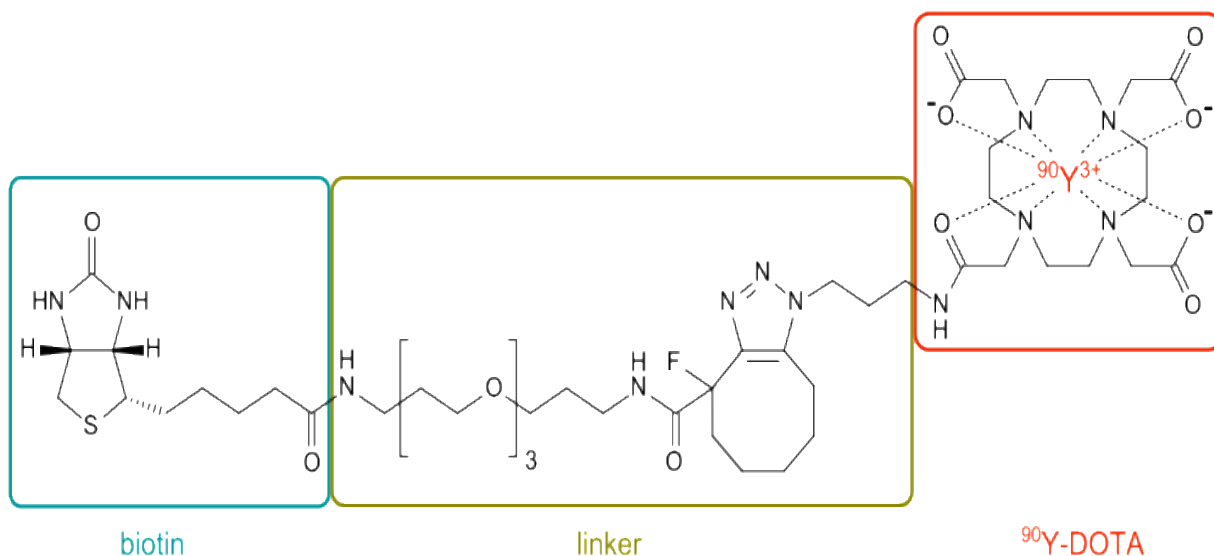
**Figure 3: Radioimmunotherapy<sup>8</sup>**



DOTA, a commonly used organic chelator, and its analogs, have been successfully used in <sup>90</sup>Y-based peptide receptor radionuclide therapy targeting neuroendocrine, prostate and other cancers. The structure of DOTA is established in figure 4. However, because of high metabolism in the liver the effectiveness of peptide receptor radionuclide therapy of HCC based on DOTA radiobioconstructs has not been reported<sup>8</sup>. There are other draw backs in utilizing DOTA as a chelator. It has been shown to lack selectivity of metals, leaving room for potential interference by other metals naturally found within the body. The formation of the DOTA complex is also known to be kinetically slow, and there is much work that needs to be done in order to improve the efficacy of the compound<sup>10</sup>. Also, being a compound not naturally found in the body, there is potential of an immune response when used. Since DOTA is commonly labeled with the radionuclide gadolinium, people who suffer from renal insufficiency cannot filter gadolinium from their body, and thus cannot undergo this form of treatment<sup>9</sup>. This is of great concern as

recently there are increases in the amount of people claiming to have “gadolinium deposition disease.” These patients experience burning, numbness, weakness, and trouble breathing post-MRI. Clearly, a new chelator for lanthanide-based theranostics of HCC is needed.

**Figure 4: DOTA Radiobioconstruct<sup>9</sup>**



Knowing this, the Korendovych lab proceeded to develop a fusion protein to serve as a chelate that directly binds <sup>90</sup>Y. We are exploring HolLEE, a Calmodulin mutant, as a novel promising candidate for an <sup>90</sup>Y chelator that could effectively treat HCC. HolLEE serves as the chelate to the HCC tumor selective antibody 2E10, forming 2E10-HolLEE. 2E10 is a commonly used antibody in HCC treatment. The single chain variable fragment (ScFv) region of the 2E10 antibody, as opposed to the entire antibody, is utilized as it can easily diffuse into tumor cells, and is less likely to cause the body to have a negative immune response<sup>12</sup>. A schematic of such isolation is provided in figure 5A. 2E10, picture in figure 5B, serves to reduce cell proliferation of HCC tumor cells through its ability to inhibit glypican-3, a proteoglycan associated with growth factors that is present on the cell membrane of HCC cells<sup>11</sup>. The advantages of this

suggested protein binding yttrium chelator include low likelihood for immunogenicity, ability to evolve to bind different metal ions tightly and selectively, as well as ease of modification. A hypothetical of HolIEE being used as a chelate is provided in figure 6. We hypothesize that HolIEE, an engineered Calmodulin mutant is a strong candidate as a novel  $^{90}\text{Y}$  chelator for use in treatment of Hepatocellular Carcinoma.

**Figure 5A: Schematic of ScFv of 2E10 isolation**    **Figure 5B: 2E10 Antibody**

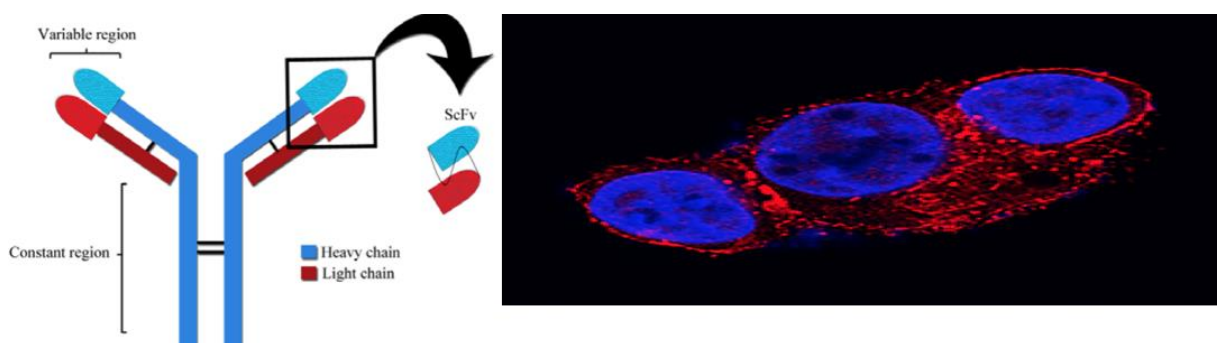
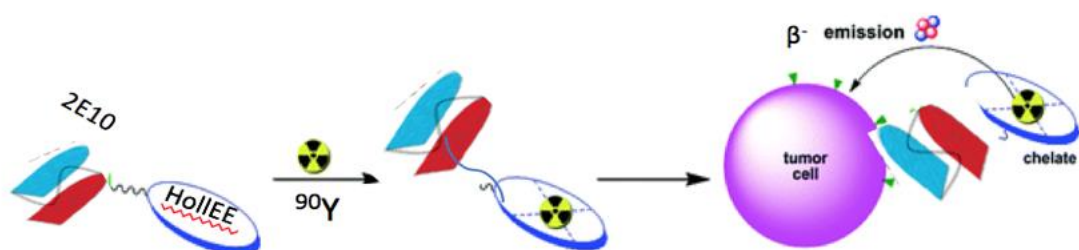


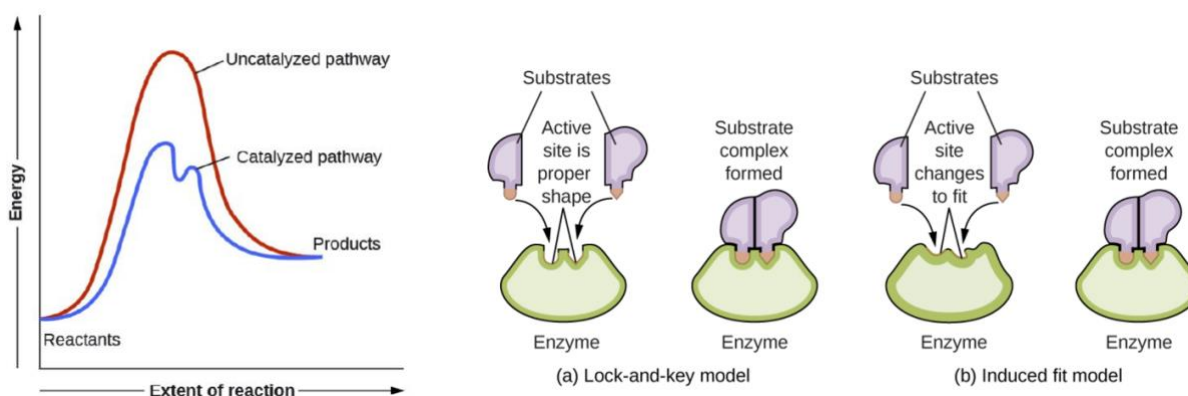
**Figure 6: HolIEE as a potential chelate**



Before delving into HolIEE and its potential as a chelate, there is some necessary background information that must be covered first in order to understand the theory behind its creation. Enzymes are catalysts composed of amino acids. They are characterized by their ability to lower the activation energy of a reaction, in turn making the reaction more kinetically favorable for substrate binding without changing the thermodynamic properties of the reaction or

being consumed, as seen in figure 7<sup>13</sup>. There are two current theories as to how substrate binding occurs visualized in figure 7. The original lock and key method hypothesizes that the enzyme and substrate act as a lock and key, and the door of an enzymatic reaction will only open if the appropriate substrate can bind to the active site and “unlock” the enzyme<sup>13</sup>. This theory gave way to the idea of enzyme specificity, but later models show it is not always necessarily one key that unlocks the potential of an enzyme. The induced-fit model, which suggests that upon substrate binding, the enzyme’s active site is able to conform to the substrate<sup>13</sup>. This also implied that the enzyme in turn can fit around different substrates as needed, and still be catalytically active. This property of enzymes gives us great hope in devising a chelate that can be used to bind various substrates.

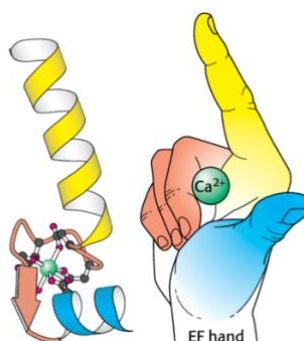
**Figure 7: Enzyme reaction coordinate and theories of substrate binding<sup>13</sup>**



Proteins that bind metal ions in order to achieve functions such as structure, electron transfer, oxygen binding, and catalysis are known as Metalloproteins. 40% of proteins within the human body can be classified as metalloproteins<sup>14</sup>. Most bind either alkali, alkaline, or transition metals, and this trend has been hypothesized to be the result of these types of metals great abundance in the environment, and thus proteins evolved to utilize these metals<sup>14</sup>. One of these proteins is calmodulin, a calcium-binding messenger protein that is present in all eukaryotic

cells<sup>4</sup>. Through its interactions with  $\text{Ca}^{2+}$ , the protein has great influence upon bodily functions such as: metabolism, apoptosis, inflammation, muscle contraction, neurotransmitter release, membrane protein organization, and cytoskeleton movement<sup>4</sup>. The structure of CaM predisposes the protein for binding to a great variety of metals. The metal binding sites consist of a pair of two lobes which are linked via alpha helix<sup>4</sup>. These lobes, labeled I-IV, each have their own EF-hands, that have two  $\text{Ca}^{2+}$  binding sites per hand<sup>4</sup>. As seen in figure 8, within each EF-hand, there is a helix-loop-helix structure, and a metal chelation loop connecting two alpha helices on its sides. The lobes each contain a large hydrophobic section vital for substrate binding. Calcium binding to the EF hands causes a structural change within CaM, exposing the hydrophobic region, and enabling it to bind to various substrates. The Korendovych Laboratory has taken the approach of modifying calcium-binding protein calmodulin to act as a scaffold for as a catalytic chelator.

**Figure 8: Binding of Calcium to the EF hand of the protein Calmodulin<sup>4</sup>**

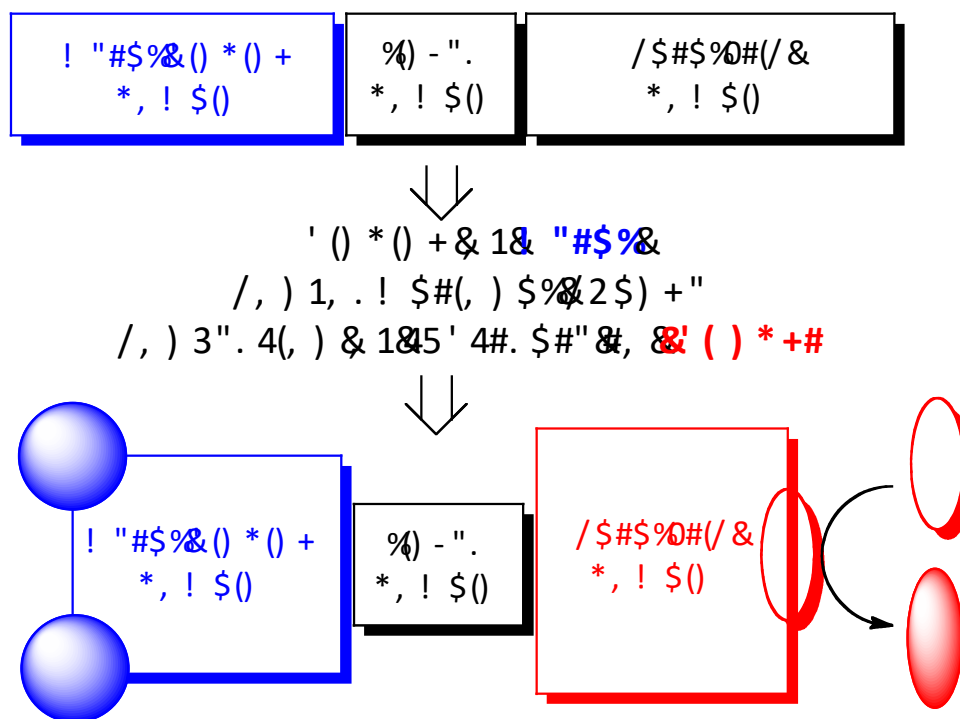


Rare earth metals, like lanthanides and yttrium, have a history of use as spectroscopic probes for determining the structure and function of CaM<sup>5</sup>. Lanthanide ions and calcium ions are similar in terms of ionic radii and hardness, and these similarities enable EF hands to have a

comparable binding affinity for lanthanides as they do for calcium. However this binding has shown problematic drawbacks<sup>3</sup>; EF-hand loop's secondary structure is ionic radius dependent, which as a result can cause perturbations to the substrate binding domain. Thus, making the EF hand a difficult framework to facilitate precise molecular engineering of a functional lanthanide binding protein<sup>5</sup>.

While there are a bevy of assays present for common earth metal like calcium, rarer metals like yttrium and lanthanides have proven to be difficult to detect in solution. In order to combat this, the Korendovych lab has applied a model of linking successful metal binding to the catalytic properties of enzymes. In theory, upon binding of metal ion co-factors, in our interest yttrium and lanthanides, to allosteric domains this creates an active site for substrate binding. Substrate binding then induces catalysis. This catalysis can then be measured and equated to the ability of the protein in question to bind a certain ion, and also become functional.

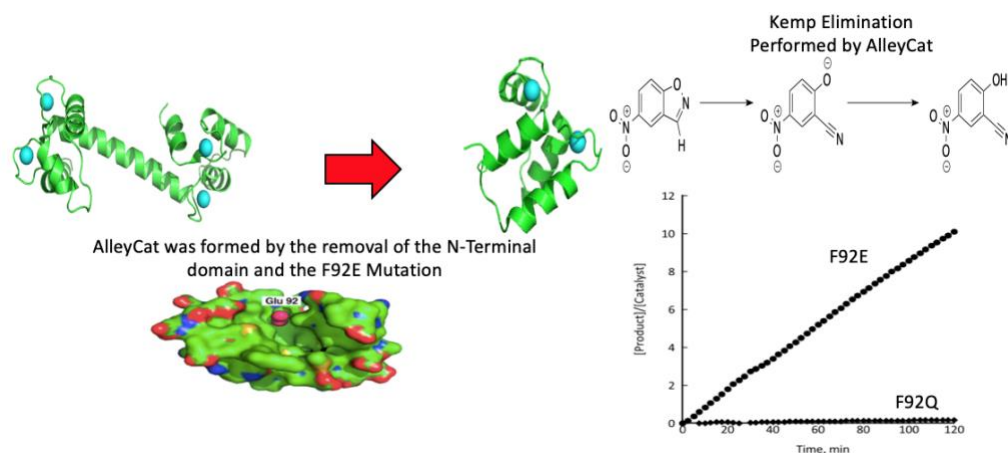
**Figure 9: Metal binding directly links to catalytic activity**





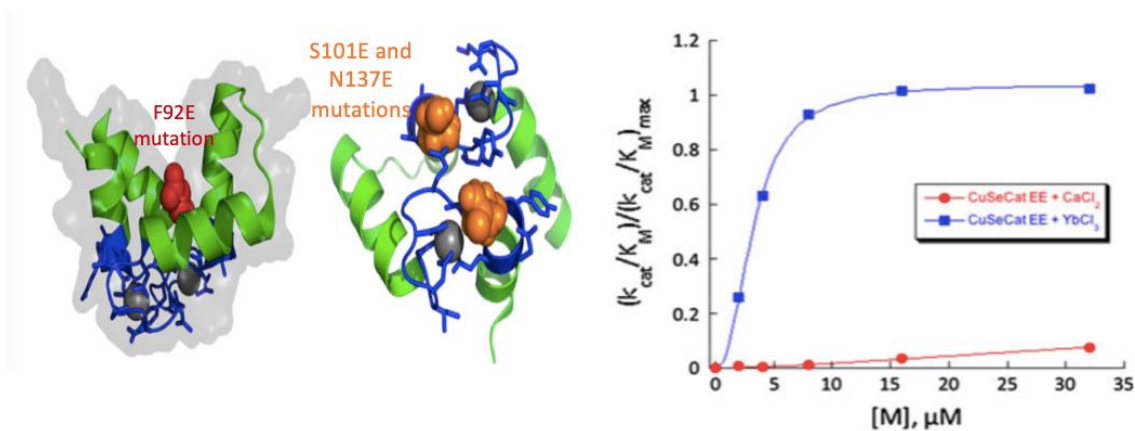
This platform for allosteric regulation, seen in figure 9, was first applied in 2010 when Ivan Korendovych designed an Allosterically Controlled Catalyst, referred to as AlleyCat, utilizing calmodulin as the scaffold<sup>2</sup>. Calmodulin was modified into an evolvable enzyme capable of performing a foreign reaction known as kemp elimination with calcium acting as the substrate by which the reaction proceeds. Kemp elimination is a useful tool in protein engineering, as through the presence of a basic catalytic residue that is capable of breaking one of the C-H bonds in a manner as seen in figure 10, this allows for the formation of a nitrile that can be detected easily by way of spectroscopic analysis at 380 nm<sup>2</sup>. Since kemp elimination is an unnatural function of calmodulin, catalytic properties observed through analysis are the result of novel mutations to the protein. Catalytic properties arose in the mutant AlleyCat through the removal of the N-terminal domain, and the mutation at position 92 of phenylalanine to glutamate, all while maintaining its ability to bind calcium<sup>2</sup>. Since the detectable kemp elimination only occurs if the Alleycat binds calcium, the Korendovych lab has used the protein as a template, exploiting the potential of its allosteric properties in hopes of further developing customizable metal sensors and chelates.

**Figure 10: AlleyCat<sup>2</sup>**

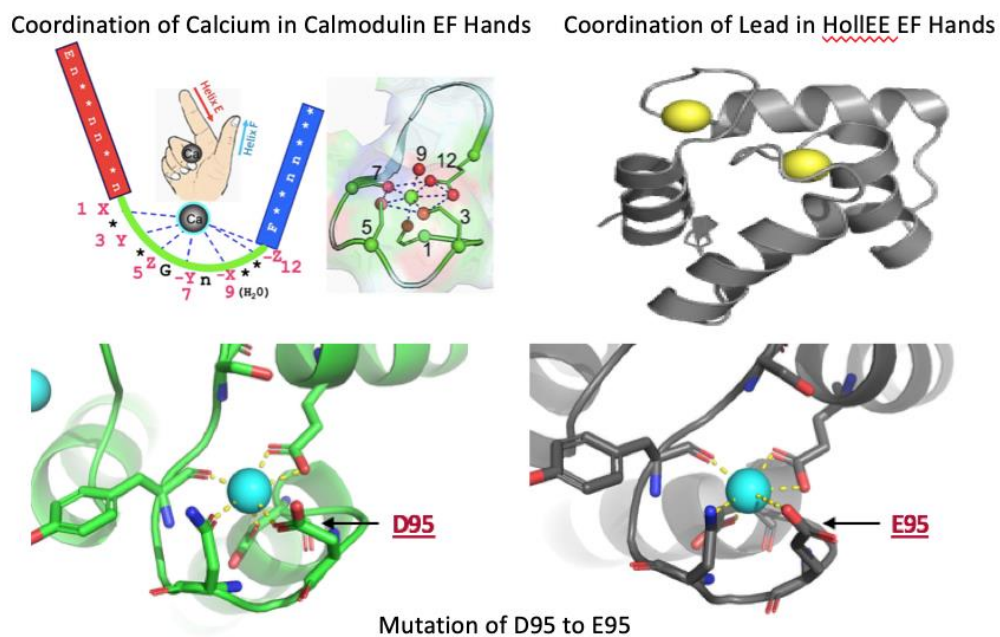


The first foray into the territory of Alleycat being able to bind metals other than calcium occurred in 2013, with the derivative nicknamed CuSeCat, standing for Customizable Sensor aided by CATalysis. Lanthanide ions being trivalent, have a similar ionic radii to calcium, and have been found to bind similarly to calmodulin, but there are seldom methods for detecting these ions in solution. CuSeCat was developed as a lanthanide sensor to selectively bind lanthanide ions while rejecting calcium through the increasing the negative charge of the metal binding loop, in positions S101 and N137, by changing both Serine and Asparagine to Glutamates<sup>1</sup>. While it was successful in performing the Kemp elimination binding to Ytterbium, CuSeCat activity increased greatly as calcium concentrations increased<sup>1</sup>. This unfortunately meant CuSeCat could not serve as an in vivo sensor or chelate due to potential interference with calcium. In figure 11, the green ribbon represents the structure of CuSeCat, the blue sticks represent the active residues in the metal binding site, the red spheres represent the F92E mutation responsible for Kemp elimination, the orange spheres represent the S101E and N137E mutations that were introduced to CuSeCat, and the gray spheres represent a trivalent metal ion.

**Figure 11: CuSeCat**



It was previously discovered that residues 1, 3, and 5 of calmodulin are directly involved in binding calcium ions. Prior work in our lab has showed that residue 5 mutations result in proteins that are completely inactive and residue 1 is essential for protein structure, thus in the creation of HolIEE mutations in position 3 of the scaffold provided by CuSeCat were made. The crystal structures of calmodulin bound to calcium vs lead, at residue 3 showed a difference of 0.6 angstroms between the two ions, indicative of the selectivity against calcium that was desired. AlleyCat7, the most active version of the AlleyCat series to date, was used as a DNA template for all mutations, and used to mimic CuSeCat. Preliminary data of HolIEE showed that mutating the aspartates in the 95 and 131 positions into glutamate of the through site-directed mutagenesis nearly eliminated activity of the protein in the presence of calcium. HolIEE showed significant activity in yttrium when compared to calcium, and thus became our potential chelator for yttrium and lanthanides. Through site-directed mutagenesis of the D95 and D131 sites of the EF-hands, which normally coordinate strongly with calcium, it is hoped that an increased affinity for lanthanide ions and/or a decreased affinity for calcium ions will be displayed while attaching within the standard calcium binding architecture. Figure 12 provides detailed images of these mutations, and figure 13 shows the preliminary data. This mutation should enable Kemp elimination in the presence of the following lanthanides and yttrium: lanthanum, cerium, praseodymium, samarium, gadolinium, terbium, ytterbium, and lutecium; but not in the presence of calcium. The success of lanthanide binding will be determined by means of Kemp assays and metal dependence assays.

**Figure 12: HolIEE specific mutations****Figure 13: Catalytic activity in presence of metal co-factors**

$k_{cat}/K_M (M^{-1}s^{-1})$	AlleyCat 7	HolIEE
0.1 mM $Ca^{2+}$	526	0.3
0.25 mM $Ca^{2+}$	580	1.7
0.1 mM $Pb^{2+}$	--	1.0
0.25 mM $Pb^{2+}$	286	0
0.1 mM $Y^{3+}$	190	47
0.25 mM $Y^{3+}$	102	14

## **Timeline**

The following procedures began in Fall 2017 academic year, and concluded in the Fall 2019

Academic Year.

- Site-directed Mutagenesis
- Expression of Ac7 Mutants
- Kinetic Assays
- Metal Dependence Assays
- pH Profile Assays
- Circular Dichroism Studies

## Methods

### *Site-directed mutagenesis*

AlleyCat7 gene was previously cloned into pEXP5-NT expression vector (Invitrogen). Both plasmids contain an N-terminal His6-tag separated from the gene of interest by a Sumo protease.

The appropriate mutation of aspartate to glutamate in the D95 and D131 positions were made using a standard mutagenesis protocol for iProof High-Fidelity DNA Polymerase, which was provided by the manufacturer (NEB). After PCR, the template was digested with DpnI restriction enzyme (NEB) and transformed into *E. coli* XL-10 cells. DNA was extracted from colonies using EZ-10 Spin Column Plasmid DNA kit and mutated sequences were confirmed by Genescript using Sanger sequencing technique.

### *Protein Expression and Purification*

The pEXP5-NT vectors containing the genes of interest were transformed into *E. coli* BL21(DE3) pLysS cells, and were then expressed using LB broth. When cells reached an OD<sub>600</sub> of ~0.5, IPTG was added to a final concentration of 0.5 mM and the temperature was lowered to 30 °C. After four hours, cells were collected by centrifugation, then stored at -80 °C until needed.

Resuspension of the Cell Pellet occurred in lysis buffer containing 25 mM HEPES, 20 mM imidazole, 0.5 mM PMSF, and 300 mM NaCl (pH 8). Cells were lysed by sonication, and then the crude cell lysate was centrifuged at 20,000xg for 1 h. The supernatant was applied to a Ni-NTA column and washed with lysis buffer (without PMSF). The protein was then eluted with buffer containing 25 mM HEPES, 250 mM imidazole, and 300 mM NaCl (pH 8). The sample was exchanged into buffer containing 50 mM Tris, 75 mM NaCl (pH 8) by applying it onto a Bio-Rad 10 DG desalting column.

### ***Removal of His-tag***

Sample was incubated with 1.0 mM DTT, 0.5 mM EDTA, and Sumo protease at a 200:1 ratio overnight at 30 °C. To ensure integrity, cleavage solution was purified using sterile technique and a 0.22  $\mu\text{M}$  PES filter before incubation.

After incubation, DTT and EDTA were removed by applying sample onto a Bio-Rad 10 DG desalting column with 50mM Tris, 75 mM NaCl (pH 8) buffer. Desalted samples were then applied to Ni-NTA column equilibrated with same buffer and allowed to sit on column for a minimum of one hour. Afterwards, protein was collected in flow through and wash and the presence of protein was determined using UV-Vis spectroscopy.

To thoroughly remove metal, approximately 5 equivalence of EDTA was added to the collected fractions. The sample was then exchanged into 20 mM MOPS (pH 7) twice using a Bio-Rad 10 DG desalting column to ensure removal of excess calcium ions and EDTA.

The purity of the protein was established by SDS-Page using a 15% acrylamide gel with Unstained Precision Protein Plus ladder (BioRad). Protein concentration was determined using UV-Vis spectroscopy where  $\epsilon_{280} = 2967 \text{ cm}^{-1}\text{M}^{-1}$ .

### ***Kinetic Assays***

Kinetic measurements were done with either a Thermo Lab-systems Multiskan Spectrum Platereader or a BioTek Eon Micro Platereader monitoring the absorbance at 380 nm at 22 °C for 5 minutes, taking measurements at every 15 second interval. The final protein concentration (determined by UV-Vis spectroscopy using  $\epsilon_{280} = 2967 \text{ M}^{-1} \text{ cm}^{-1}$ ) for kinetic measurements was 5.0  $\mu\text{M}$ . Final substrate concentrations ranged from 0.12 to 0.96 mM. Final metal ion concentration was 100  $\mu\text{M}$ . Kinetic parameters ( $k_{\text{cat}}$  and  $K_{\text{M}}$ ) were obtained by fitting the linear portion of data

to the Michaelis-Menten equation:  $\{v_0 = k_{cat}[E]_0[S]_0/(K_M + [S]_0)\}$  using Kaleidagraph 4.5 (Synergy Software).

### ***Metal Dependence Assays***

Kinetic measurements were done with either a Thermo Lab-systems Multiskan Spectrum Platereader or a BioTek Eon Micro Platereader monitoring the absorbance at 380 nm at 22 °C for 5 minutes, taking measurements at every 15 second interval. Final substrate concentration was 0.6 mM Kemp substrate. The final protein concentration (determined by UV-Vis spectroscopy using  $\epsilon_{280} = 5445 \text{ M}^{-1} \text{ cm}^{-1}$  for uncut protein and  $\epsilon_{280} = 2967 \text{ M}^{-1} \text{ cm}^{-1}$  for cut protein) for kinetic measurements was 2.5  $\mu\text{M}$ . Final metal concentrations ranged from 0 to 250  $\mu\text{M}$ . In addition, a concentration of 15  $\mu\text{M}$  EDTA was used to establish activity without metal ions present.

### ***pH Profile Assays***

Kinetic measurements were done with either a Thermo Lab-systems Multiskan Spectrum Platereader or a BioTek Eon Micro Platereader monitoring the absorbance at 380 nm at 22 °C for 5 minutes, taking measurements at every 15 second interval. Final substrate concentration was 0.6 mM Kemp substrate. Final metal ion concentration was 100  $\mu\text{M}$ . The extinction coefficient of 15,800  $\text{cm}^{-1}\text{M}^{-1}$  was used to determine product concentration at pH 5.5 and above. At pH 4.5 and 5.0, the product coefficients of 12,480  $\text{cm}^{-1}\text{M}^{-1}$  and 14,220  $\text{cm}^{-1}\text{M}^{-1}$ , respectively, were used. Samples were run in acetate buffer (pH 4.5-5.5), MES (pH 6.0-6.5), HEPES (pH 7.0-7.5), and Tris (pH 8.0-8.5) with concentrations of 50 mM. The final protein concentration (determined by UV-Vis spectroscopy using  $\epsilon_{280} = 5445 \text{ M}^{-1} \text{ cm}^{-1}$  for uncut protein and  $\epsilon_{280} = 2967 \text{ M}^{-1} \text{ cm}^{-1}$  for cut protein) for kinetic measurements was 5.0  $\mu\text{M}$ . The curves were fit to



$\{(k_{cat}/K_M)_{max}=(k_{cat}/K_M)_{protonated}+(k_{cat}/K_M)_{deprotonated} \times 10^{-pK_a}/(10^{-pH}+10^{-pK_a})\}$ , where  $pK_a$  is the apparent  $pK_a$  value of the active residue, using Kaleidagraph 4.5 (Synergy software).

### ***Circular Dichroism***

The CD spectra were collected on the Jasco J-715 CD spectrometer, using a step scan mode (4 sec averaging time) averaging over three runs, using a quartz cuvette with a 0.1 cm path length. Each samples contained 4 mM MOPS with 25  $\mu$ M concentration of protein. Samples consisted of varying amounts of metal chloride salts.

Care was taken so the sample absorbance never exceeded 1.5 at all wavelengths to produce reliable ellipticity values.

### ***Michaelis-Menten equation***

The Michaelis-Menten equation determines the reaction velocity ( $v_0$ ) by the product turnover per unit time ( $k_{cat}$ ), the initial concentration of enzyme ( $[E]_0$ ), the concentration of substrate ( $[S]$ ), and the concentration of substrate when the reaction is at half of its maximal velocity ( $K_M$ ). Maximal velocity ( $v_{max}$ ) of the enzyme is determined by way of multiplying product turnover and concentration of the enzyme.

$$v_0 = \frac{k_{cat}[E]_0[S]}{K_M + [S]} = \frac{v_{max}[S]}{K_M + [S]}$$

## Experimentals

The D95 and D131 sites of AlleyCatR7 were mutated from aspartate to glutamate via site-directed mutagenesis in order to reject calcium binding and introduce a preference for lanthanide ions. This site-directed mutagenesis was done prior to my addition to the project. By way of Ni-NTA column chromatography, the mutated protein product, HolIEE, was expressed and purified. SDS-PAGE analysis was conducted to confirm the purity of the protein. After protein expression and purity was confirmed, the removal of the N-terminal His6-tag was conducted via Sumo protease cleavage, success of this removal was confirmed by SDS-Page. The process of protein expression, purification, and removal of the His6-tag was conducted as needed.

**Figure 14: Metal Dependence Assay data**

Concentration of Metal [uM]	Ca ( $k_{cat}/K_M$ $M^{-1} s^{-1}$ )	Gd ( $k_{cat}/K_M$ $M^{-1} s^{-1}$ )	Ce ( $k_{cat}/K_M$ $M^{-1} s^{-1}$ )	La ( $k_{cat}/K_M$ $M^{-1} s^{-1}$ )	Lu ( $k_{cat}/K_M$ $M^{-1} s^{-1}$ )	Nd ( $k_{cat}/K_M$ $M^{-1} s^{-1}$ )	Sm ( $k_{cat}/K_M$ $M^{-1} s^{-1}$ )	Tb ( $k_{cat}/K_M$ $M^{-1} s^{-1}$ )	Y ( $k_{cat}/K_M$ $M^{-1} s^{-1}$ )	Pr ( $k_{cat}/K_M$ $M^{-1} s^{-1}$ )	Yb ( $k_{cat}/K_M$ $M^{-1} s^{-1}$ )
0	-0.14138	-0.021371	0.0049318	-0.032879	-0.064113	0.055893	-0.067401	0.042742	-0.016439	0.011507	0.027947
5	-0.23344	0.12987	0.098636	19.97	-0.019727	0.065757	-0.019727	0.10521	13.137	0.031235	0.04603
10	0.14220	0.19727	-0.05014	63.839	2.1371	52.892	68.664	0.71593	35.837	53.12	-0.082196
20	-0.014795	0.27782	0.23015	103.99	28.708	161.02	177.84	6.0266	85.387	162.36	-0.067401
40	0.093704	31.419	0.10521	142.83	74.927	196.42	172.74	104.22	139.7	175.95	21.84
80	-0.034522	69.078	20.066	151.02	102.38	173.77	163.32	110.8	161.83	180.14	87.674
100	0.0032879	72.349	36.102	146.08	112.06	179.07	146.42	105.7	161.91	177.16	82.91
250	0.0031289	68.422	130.64	139.68	27.661	123.52	91.659	78.714	96.336	120.88	75.05

Metal Dependence assays for 2.5  $\mu$ M HolIEE were conducted at a wavelength of 380 nm at 22 °C analyzing  $k_{cat}/K_M$  for the following final concentrations of each lanthanide ion: 0, 5, 10, 20, 40, 80, 100, and 250  $\mu$ M. Measurements were taken every 5 minutes, at 15 second intervals

using a BioTek Eon Micro Platereader. Substrate concentration for this reaction was 0.6 mM Kemp. High levels of catalytic activity upon ion binding were expressed by the following ions and concentrations as seen in figure 14: Cerium (250  $\mu$ M), Lanthanum (20  $\mu$ M-100 $\mu$ M), Neodymium (20  $\mu$ M-250 $\mu$ M), Samarium (80  $\mu$ M, 250 $\mu$ M), Terbium (40  $\mu$ M-250 $\mu$ M), Yttrium (20  $\mu$ M-40 $\mu$ M), and Praseodymium (20  $\mu$ M-250 $\mu$ M). Moderate levels of catalytic activity upon ion binding were expressed by Gadolinium (80  $\mu$ M, 250 $\mu$ M), Lutetium (100  $\mu$ M, 250 $\mu$ M), and Ytterbium (80  $\mu$ M, 250 $\mu$ M) as seen in figure 14.

**Figure 15: pH Profile Assay Data**

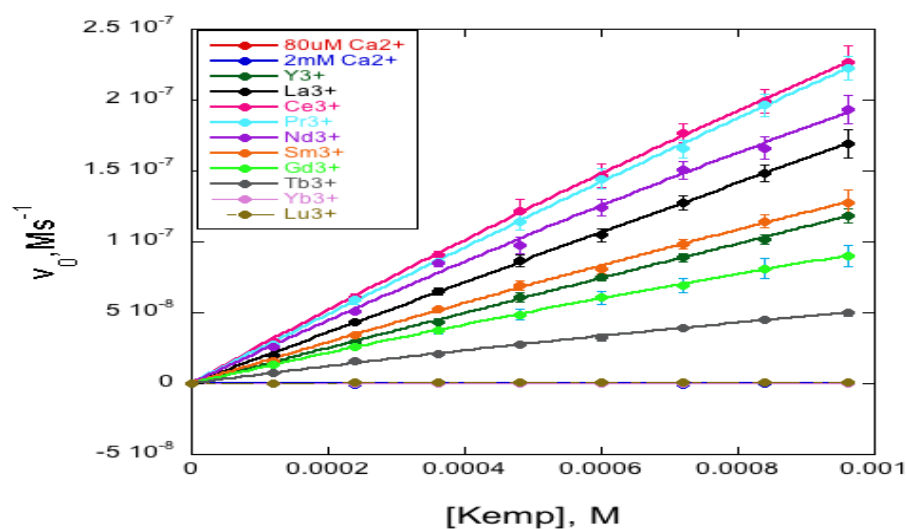
pH of Buffer	Ca ( $k_{cat}/K_M$ $M^{-1} s^{-1}$ )	Y ( $k_{cat}/K_M$ $M^{-1} s^{-1}$ )	La ( $k_{cat}/K_M$ $M^{-1} s^{-1}$ )	Pr ( $k_{cat}/K_M$ $M^{-1} s^{-1}$ )	Nd ( $k_{cat}/K_M$ $M^{-1} s^{-1}$ )	Sm ( $k_{cat}/K_M$ $M^{-1} s^{-1}$ )	Gd ( $k_{cat}/K_M$ $M^{-1} s^{-1}$ )	Tb ( $k_{cat}/K_M$ $M^{-1} s^{-1}$ )	Yb ( $k_{cat}/K_M$ $M^{-1} s^{-1}$ )	Lu ( $k_{cat}/K_M$ $M^{-1} s^{-1}$ )	Ce ( $k_{cat}/K_M$ $M^{-1} s^{-1}$ )	Lu ( $k_{cat}/K_M$ $M^{-1} s^{-1}$ )
5	-0.24134	15.337	-9.7192	2.7203	8.3143	1.3754	9.62	7.3717	0.98343	3.3309	-8.2788	-8.2788
5.5	0.039043	6.5032	12.36	32.187	22.466	5.8963	24.146	15.295	1.9878	14.133	1.7363	1.7363
6	0.031481	93.354	82.859	40.254	109.79	43.891	55.106	60.146	15.931	31.115	9.7006	9.7006
6.5	-40.75	119.82	116.37	2.1239	113.46	61.953	20.389	78.661	50.578	4.4117	52.477	52.477
7	0.028645	13.804	123.96	126.32	126.74	70.364	12.842	26.131	51.823	37.617	78.762	78.762
7.5	0.080141	24.176	122.49	156.15	120.37	52.837	1.7857	39.884	8.9466	32.188	107.7	107.7
8	0.038714	31.204	22.916	132.1	102.99	11.102	48.756	23.318	0.84901	11.862	80.18	80.18
8.5	-0.38114	0.46309	17.251	-0.51907	-0.39693	-0.86758	0.23031	-0.032879	-0.36758	-0.17771	45.443	45.443

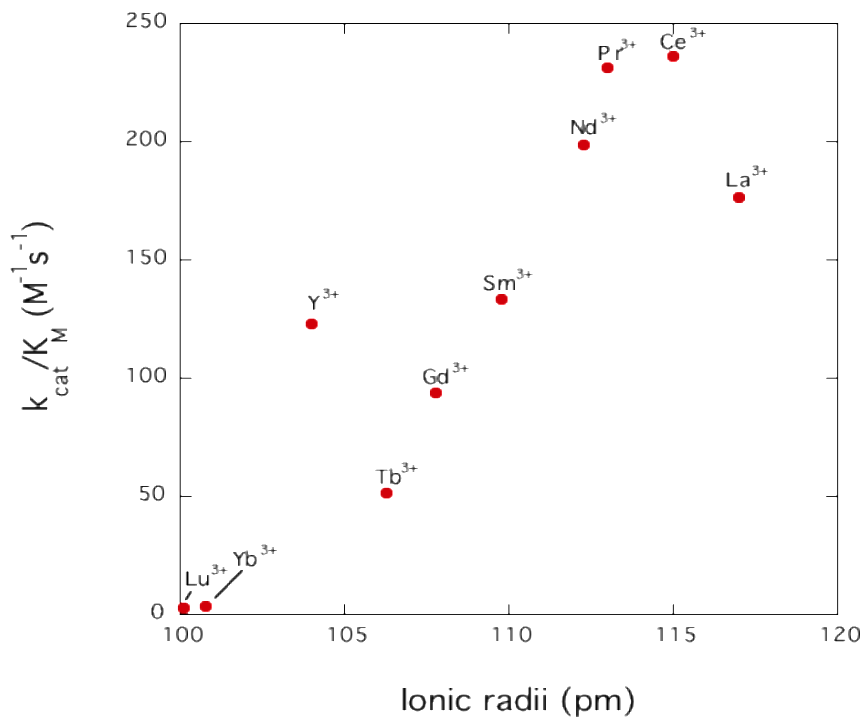
pH Profile assays for 5.0  $\mu$ M HolIEE were conducted at a wavelength of 380 nm at 22  $^{\circ}$ C

analyzing  $k_{cat}/k_M$  in the following buffer solutions and pH values: acetate buffer (pH 4.5-5.5), MES (pH 6.0-6.5), HEPES (pH 7.0-7.5), and Tris (pH 8.0-8.5). Lanthanide ion concentration and Kemp substrate concentration utilized were 100  $\mu$ M and 0.6 mM Kemp. High levels of catalytic activity upon ion binding were expressed by the following ions and pH levels as seen in figure 4: Yttrium (pH 6- 7), Lanthanum (pH 6-7.5), Praseodymium (pH 6-8), Neodymium (pH 6-

8), Samarium (pH 6.5, 7), Terbium (pH 6.5), Lutetium (pH 6), and Cerium (pH 7-8). Moderate levels of catalytic activity upon ion binding were expressed by the following ions and pH levels as seen in figure 15: Yttrium (pH 7.5, 8), Praseodymium (pH 5.5), Neodymium (pH 5.5), Samarium (pH 6, 7.5), Gadolinium (pH 5.5-6.5, 7.5), Terbium (pH 6, 7-8), Ytterbium (pH 6.5, 7), Lutetium (pH 6.5-7), Cerium (pH 7, 8.5). The pH profile results seen in figure 15 were inconclusive, and we were not able to determine HolLEE-lanthanide ion binding efficiency from them.

**Figures 16: Kinetic Assay Data of HolLEE**



**Figure 17: Relationship between Ionic Radius and Catalytic Activity**

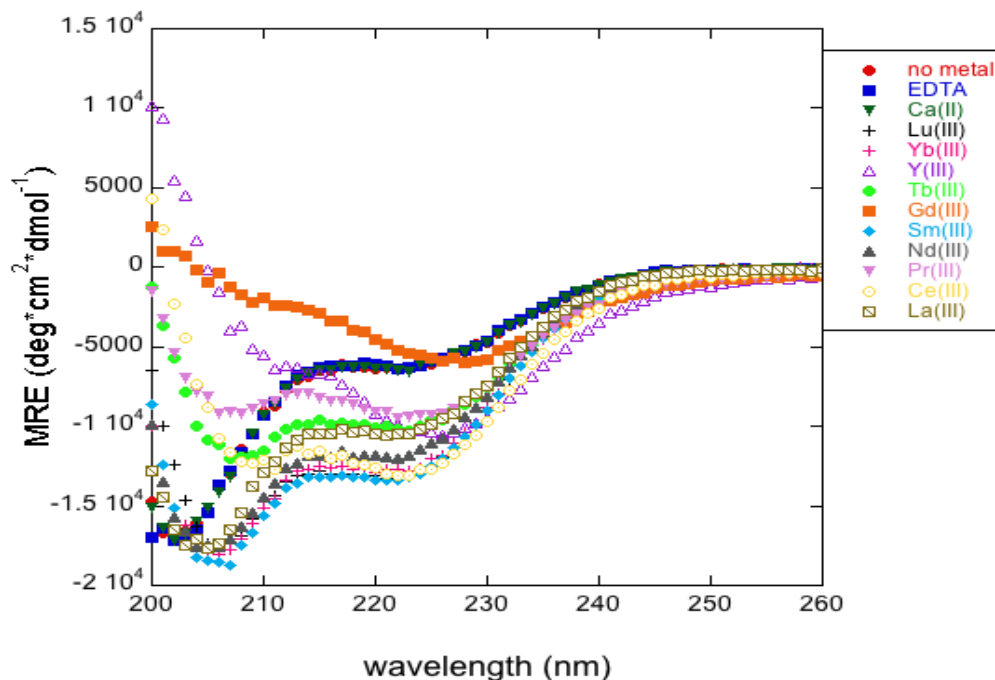
	2mM Ca <sup>2+</sup>	Ca <sup>2+</sup>	Y <sup>3+</sup>	La <sup>3+</sup>	Ce <sup>3+</sup>	Pr <sup>3+</sup>	Nd <sup>3+</sup>	Sm <sup>3+</sup>	Gd <sup>3+</sup>	Tb <sup>3+</sup>	Yb <sup>3+</sup>	Lu <sup>3+</sup>
$k_{cat}/K_M$ ( $M^{-1}s^{-1}$ )	0.03	0.03	123	176	236	231	199	133	94	52	3.7	2.9

HolLEE's ability to perform kemp elimination was analyzed by assessing the Michaelis-Menten Kinetics in the presence of lanthanides ions and yttrium. Conducted at a wavelength of 380 nm at 22 °C , pH 7.0 with 0.08 mM metal, and 1.0mM HolLEE, measurements were taken every 5 minutes, at 15 second intervals using a BioTek Eon Micro Platereader. Even when exposed to physiological levels of calcium, HolLEE still showed selectivity for lanthanide ions. We see the kinetic assay data in figure 17 shows that HolLEE expresses the most activity in

decreasing order for Cerium, Praseodymium, Neodymium, Lanthanum, Samarium, and Yttrium.

There is also a noted general trend of increased activity with increased ionic radius.

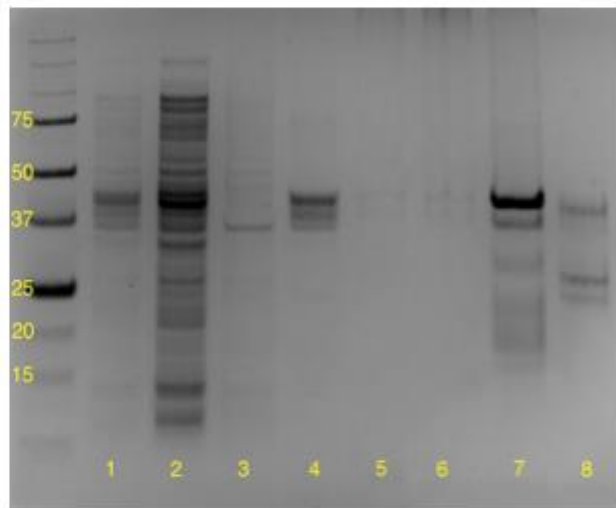
**Figure 18: CD Spectra of HolE**



CD Spectra was collected lanthanide ions and yttrium; in order to show protein ion binding occurring in respect to the negative control of Calcium in figure 18. Each ion sample was processed by the Jasco J-715 CD spectrometer at a wavelength range of 200nm to 260nm, using a step scan mode (4 sec averaging time) averaging over three runs, using a quartz cuvette with a 0.1 cm path length. Samples contained 4 mM MOPS with 25  $\mu$ M concentration of protein, and were treated with .08mM metal

**Figure 19: Isolation of 2E10-HolIEE**

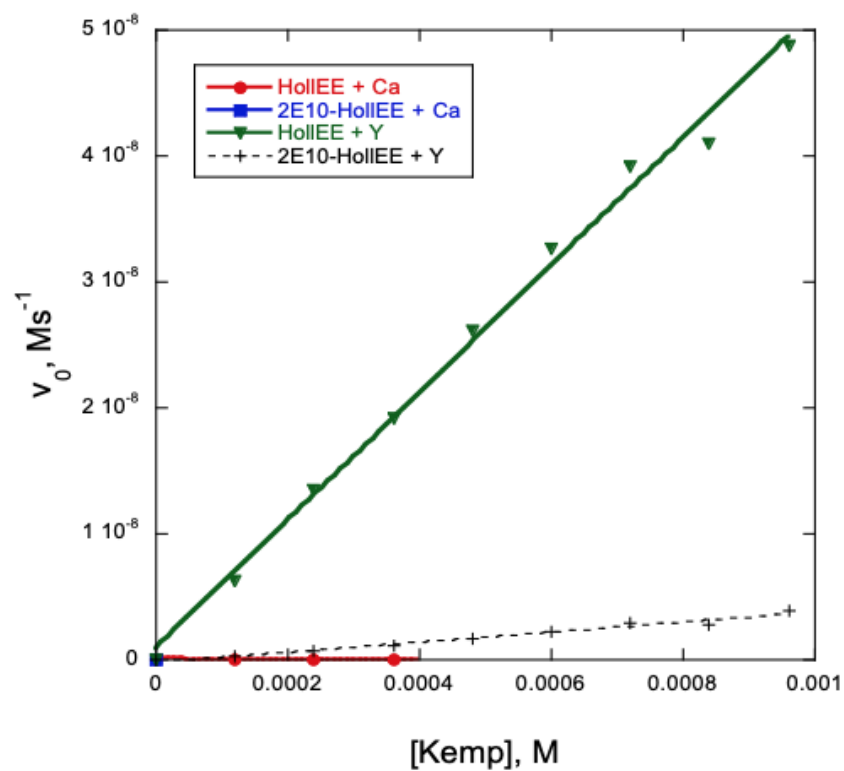
## 2E10-HolIEE



Lane 1) cells before induction, 2) cell pellet before purification, 3) supernatant after sonication, 4) supernatant before loading onto Ni-NTA column, 5) Ni-NTA column flow through, 6) Ni-NTA column wash, 7) uncut 2E10-HolIEE before TEV cleavage, 8) 2E10-HolIEE after incubation overnight with TEV

In order to confirm the successful conjugation of the anti-body 2E10 and our protein HolIEE, SDS-PAGE analysis was performed. Samples were taken from cells prior to induction and purification, the supernatant after sonication and prior to being loaded on the Ni-NTA column, column flow through and wash, as well as before and after TEV cleavage. As seen in lane 8 of figure 19, pure 2E10-HolIEE was isolated, and able to be utilized for testing.

**Figure 20: Kemp elimination capability of 2-E10 HolIEE versus HolIEE  
in presence of calcium and yttrium**

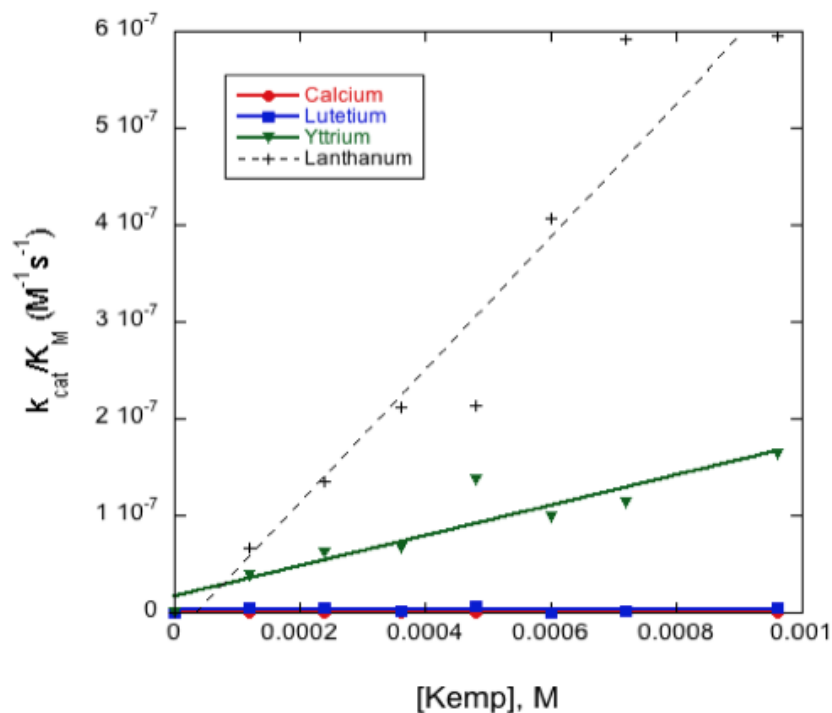


Kemp elimination using 2E10-HolIEE (0.5 mM) in the presence of yttrium (0.08 mM) and calcium (0.08 mM) in 20 mM MOPS, 100 mM NaCl, pH 7.0.

$k_{cat}/K_M$	
2E10-HolIEE	$8.0 \text{ M}^{-1}\text{s}^{-1}$
HolIEE	$101 \text{ M}^{-1}\text{s}^{-1}$



**Figure 21: Kemp elimination capability of 2-E10 HolEE in presence of calcium, yttrium, lutetium, and lanthanum**



Kemp elimination using 2E10-HolEE (0.5 mM) in the presence of yttrium (0.08 mM) and calcium (0.08 mM) in 20 mM MOPS, 100 mM NaCl, pH 7.0.

The ability of 2E10-HolEE versus HolEE to perform kemp elimination was analyzed by assessing the Michaelis-Menten Kinetics in the presence of calcium and yttrium is seen in figure 20. Conducted at a wavelength of 380 nm at 22 °C , pH 7.0 with 0.08 mM metal, and 1.0mM HolEE, measurements were taken every 5 minutes, at 15 second intervals using a BioTek Eon Micro Platereader. Non-conjugated HolEE had a higher catalytic activity with a  $k_{cat}/K_M$  of  $101 M^{-1}s^{-1}$ , in comparison to 2E10-HolEE which had a  $k_{cat}/K_M$  of  $8.0 M^{-1}s^{-1}$ . 2E10 conducted kemp

elimination in presence of calcium, yttrium, lanthanum, and lutetium under the same conditions listed previously for the 2E10-HolLEE versus HolLEE experiment, and the results can be seen in figure 21. There was a general trend of increase of catalytic activity and increase of kemp concentration in the presence of yttrium and lanthanum, with lanthanum having the highest catalytic activity. 2E10-HolLEE rejected both lutetium and calcium.

## Discussion

HolLEE's potential as a chelate was established by analyzing its ability to perform kemp elimination in the presence of lanthanides ions and yttrium. Even when exposed to physiological levels of calcium, HolLEE still showed selectivity for lanthanide ions. Calcium could not bind to HolLEE and precipitated out of solution. The kinetic assay data shows that HolLEE expresses the most activity in decreasing order for Cerium, Praseodymium, Neodymium, Lanthanum, Samarium, and Yttrium.

As we compare catalytic activity to ionic radius, there is a general trend of increased activity with increased ionic radius. Since catalytic activity of HolLEE is dependent upon the exposure of the substrate binding pocket and EF-hands positioning, larger ions up to a point are preferable substrates over smaller ions as shown through the data set in figure 17. This does not necessarily mean that the binding of HolLEE to smaller ions is weaker than that of HolLEE to larger ions, it means sensing of the smaller ions would not be as detectable by means of HolLEE catalysis in comparison to larger ions. Without metal, one can observe HolLEE display a disordered structure that is incapable of catalytic activity. Once exposed to the lanthanides, HolLEE then exhibits significant  $\alpha$ -helical structure. There also appears to be a correlation between Kemp elimination activity and the degree of alpha-helicity; as the metals that have greater activity, tend to exhibit greater mean residue ellipticity (MRE) compared to the lower activity metals, and have a more optimal ionic radius to maintain the alpha-helix. The circular dichroism data set shows that there is a direct relation between ionic radius, protein stability, and catalytic activity of HolLEE.

Once its ability to bind Yttrium was confirmed, HolLEE was then conjugated to 2E10. Post-isolation 2E10-HolLEE's metal binding was assessed in comparison to its predecessor HolLEE.

The 2E10 fusion of HolLEE proved to bind to yttrium, while completely rejecting calcium, and maintaining catalytic activity. While it was not to the same degree of non-fusion HolLEE in terms of catalytic efficacy, most likely due to antibody interference with the binding site or metal binding, 2E10-HolLEE still looks promising as a potential mean of radioembolizations. 2E10-HolLEE's catalytic activity was also tested with the Lanthanide ions Lanthanum and Lutetium, expressing great catalytic activity in Lanthanum, which has a larger ionic radius than lutetium, which expressed little catalytic activity predictably due to its inability to support the necessary alpha helix secondary structure of HolLEE as a result of its smaller ionic radius. This means HolLEE could serve as an effective chelate for other types of radionuclides.

The next step for this project will be to optimize HolLEE as a chelate for radioembolization of HCC. Testing must be completed *in vitro* to determine if 2E10-HolLEE is able to detect and/or induce a therapeutic effect against HCC, prior to moving towards an *in vivo* model. We must also further determine the binding affinity HolLEE-2E10, the proposed chelate, has for yttrium. In order to continue with the studies that prove this however, the purification method of 2E10-HolLEE must be perfected in order to achieve greater yields of the conjugated protein. HolLEE due to its affinity for a great range of lanthanide ions may also have the ability to act as a chelate for ions other than yttrium. This poses HolLEE to have application outside of the realm of HCC, and the protein could also be viable for treating different kinds of cancers. Now that there has been some headway made in confirming the *in vitro* capability of this potential  $^{90}\text{Y}$  theranostic, testing of HolLEE within an *in vivo* model is a natural and necessary next step. This would be to ensure that HolLEE maintains its displayed *in vitro* preference of  $^{90}\text{Y}$  binding affinity, even in the face of physiological levels of calcium present in a living system. Another concern that must be addressed moving forward is the stability of the radiobioconstruct's lanthanide ion binding *in vivo*. If HolLEE is unable to

maintain a strong capability to bind lanthanides *in vivo*, this poses a potential threat of poisoning the living system.

The continued success of HolIEE as an yttrium chelator is a great advance in the field of theranostic application in the treatment of HCC. The model of protein metal chelators like HolIEE is more advantageous than its predecessors in terms of creation, ability to evolve, and low risk of posing an immunogenetic threat. The *in vitro* work presented in this thesis provides a great stepping stone towards developing an effective *in vivo* model. Through the catalytic properties and stability HolIEE presents upon binding lanthanide ions, and especially yttrium, the science community comes closer than before to an effective treatment for HCC.

### Works Cited

1. Moroz, O. V. *et al.* A single mutation in a regulatory protein produces evolvable allosterically regulated catalyst of nonnatural reaction. *Angew. Chemie - Int. Ed.* 52, 6246–6249 (2013).
2. Korendovych, I. V. *et al.* Design of a switchable eliminase. *Proc. Natl. Acad. Sci.* 108, 6823–6827 (2011).
3. Mack, K. L. *et al.* Reprogramming EF-hands for design of catalytically amplified lanthanide sensors. *J. Biol. Inorg. Chem.* 18, 411–418 (2013).
4. Berg, J. M., Tymoczko, J. L. & Stryer, L. *Biochemistry. Biochemistry textbook 2015*, (W.H. Freeman and Company).
5. Am Ende, C. W., Meng, H. Y., Ye, M., Pandey, A. K. & Zondlo, N. J. Design of lanthanide fingers: Compact lanthanide-binding metalloproteins. *ChemBioChem* 2010, 11, 1738–1747.
6. Waghray, A.; Murali, A. R.; Menon, K. N., Hepatocellular carcinoma: From diagnosis to treatment. *World J Hepatol* 2015, 7 (8), 1020-9
7. Gomes, M. A., Priolli, D. G., Tralhão, J. G., Botelho, M. F., Hepatocellular carcinoma: epidemiology, biology, diagnosis, and therapies. *Rev Assoc Med Bras* 2013, 59 (5), 514-24.
8. Larson, Steven M., et al. “Radioimmunotherapy of Human Tumours.” *Nature Reviews Cancer*, vol. 15, no. 6, 2015, pp. 347–360., doi:10.1038/nrc3925.
9. Schultz, Michael K., et al. “Synthesis of a DOTA–Biotin Conjugate for Radionuclide Chelation via Cu-Free Click Chemistry.” *Organic Letters*, vol. 12, no. 10, 2010, pp. 2398–2401., doi:10.1021/ol100774p.

10. Marquez BV, Zheleznyak A, Lapi SE. Glypican-3-targeted <sup>89</sup>Zr PET imaging of hepatocellular carcinoma: where antibody imaging dares to tread. *J Nucl Med*. 2014;55(5):708-9. Epub 2014/03/26. doi: 10.2967/jnumed.113.136234. PubMed PMID: 24665087.
11. Filmus J, Capurro M. Glypican-3: a marker and a therapeutic target in hepatocellular carcinoma. *The FEBS journal*. 2013;280(10):2471-6. Epub 2013/01/12. doi: 10.1111/febs.12126. PubMed PMID: 23305321.
12. Li, Y. S., D.L.; Scholler, N.; Kaplan, D.E., Validation of glypican-3-specific scFv isolated from paired display/secretory yeast display library. *BMC Biotech* 2012, 12 (23).
13. UC Davis University of California. (2019, February 23). 4.6: Catalysis. Retrieved from [https://chem.libretexts.org/Courses/Valley\\_City\\_State\\_University/Chem\\_122/Chapter\\_4:\\_Chemical\\_Kinetics/4.6:\\_Catalysis](https://chem.libretexts.org/Courses/Valley_City_State_University/Chem_122/Chapter_4:_Chemical_Kinetics/4.6:_Catalysis)
14. Waldron, K. J.; Rutherford, J. C.; Ford, D.; Robinson, N. J., Metalloproteins and metal sensing. *Nature* 2009, 460 (7257), 823-30